

Sensitivity of the Mott Transition to Non-cubic Splitting of the Orbital Degeneracy: Application to $\text{NH}_3\text{K}_3\text{C}_{60}$

Nicola Manini^{1,2,3,4*}, Giuseppe E. Santoro^{3,4†},
Andrea Dal Corso^{3,4‡}, and Erio Tosatti^{3,4,5§}

¹ *Dip. Fisica, Università di Milano, Via Celoria 16 - 20133 Milano, Italy*

² *INFM, Unità di Milano, Milano, Italy*

³ *INFM, Unità Trieste SISSA, Italy*

⁴ *International School for Advanced Studies (SISSA),
Via Beirut 4, I-34013 Trieste, Italy*

⁵ *International Centre for Theoretical Physics (ICTP),
P.O. Box 586, I-34014 Trieste, Italy*

(21-12-2001)

Within dynamical mean-field theory, we study the metal-insulator transition of a twofold orbitally degenerate Hubbard model as a function of a splitting Δ of the degeneracy. The phase diagram in the $U - \Delta$ plane exhibits two-band and one-band metals, as well as the Mott insulator. The correlated two-band metal is easily driven to the insulator state by a strikingly weak splitting $\Delta \ll W$ of the order of the Kondo-peak width zW , where $z \ll 1$ is the metal quasiparticle weight. The relevance of this result to the insulator-metal transition in the orthorhombic expanded fulleride $\text{NH}_3\text{K}_3\text{C}_{60}$ is discussed.

I. INTRODUCTION

Strong electron correlations in multi-band, orbitally degenerate systems represent an important current theoretical challenge. A lively experimental playground for that is provided by electron- and hole-doped fullerene systems, which exhibit a variety of behavior, including unconventional metals like cubic CsC_{60} [1], superconductors of the A_3C_{60} family ($\text{A} = \text{K}, \text{Rb}, \text{Cs}$) [2], superconducting FET devices [3,4], and insulators, presumably of the Mott-Jahn-Teller type [5,6]. Among them we can place A_4C_{60} [7], Na_2C_{60} [8] and the class of compounds $\text{NH}_3\text{K}_3\text{C}_{60}$, $\text{NH}_3\text{K}_2\text{RbC}_{60}$, $\text{NH}_3\text{KRb}_2\text{C}_{60}$, as well as $\text{NH}_3\text{Rb}_3\text{C}_{60}$ [9–11]. In these ammoniated compounds, insertion of the electronically inert NH_3 molecules acts to expand the C_{60} lattice, turning the cubic, metallic and superconducting state of K_3C_{60} into an orthorhombic narrow-gap antiferromagnetic insulator [9,10,12]. In this transition, the increase in volume per C_{60} molecule relative to K_3C_{60} , with its probable slight decrease of electron effective bandwidth W , is believed to play an important role, as confirmed by the recently demonstrated pressure-induced reversion to a fully metallic and superconducting – while still orthorhombic – phase [13,14].

Nonetheless, a possible role of the crystal-structure anisotropy in this Mott transition – a transition generally believed to occur more readily for reduced orbital degeneracy [15,16], cannot be excluded. It has even been proposed that precisely the splitting of degeneracy [17] induced by the orthorhombic distortion could be the crucial ingre-

*E-mail: nicola.manini@mi.infm.it

†E-mail: santoro@sissa.it

‡E-mail: dalcorso@sissa.it

§E-mail: tosatti@sissa.it

dient driving the transition from the metal and superconductor to the insulator [10]. Earlier work showed the Mott transition in d -orbitally degenerate lattice models to take place at larger values of U/W for larger degeneracy, roughly proportionally to \sqrt{d} [6,15,16,18,19]. A strong enough “crystal-field” splitting of the threefold degenerate t_{1u} molecular orbital of C_{60} caused by orthorhombic anisotropy could remove one or several bands away from the Fermi level, effectively reducing the orbital degeneracy d , thus shifting the Mott transition to a smaller critical value U_c/W . Exploring this concept, the basic question is how strong the splitting must be to promote such an effective reduction of degeneracy. In a non-interacting system, that reduction would clearly require a splitting magnitude similar to or larger than the full electron bandwidth W . In a strongly interacting systems, it is important to understand whether influencing the metal-insulator transition will again require anisotropic splittings as large as the bandwidth, or else if some smaller energy scale will emerge in its place.

In this paper we exploit dynamical mean field theory (DMFT) to answer this question, studying the effects of a band splitting on the Mott transition of an orbitally degenerate, strongly correlated metal. For that purpose we adopt the simplest idealization, namely a $d = 2$ orbitally degenerate Hubbard model with bandwidth W and on-site repulsion U , and mimic the noncubic anisotropy by a diagonal splitting Δ between the two bands. In this model, we study the $T = 0$ phase diagram in the (U, Δ) plane, and examine in particular how the Mott transition is influenced by the splitting.

The main result found is that the effect is remarkably strong at large U , where the anisotropy-induced transition between the correlated multi-band metal and the Mott insulator takes place very readily, in fact for $\Delta \ll W$. We interpret that as follows. The metallic band, originally of width W , is renormalized in the strongly correlated metal into a narrower “Kondo-like” quasiparticle peak of width zW , with $1 \gg z \rightarrow 0$ as $U \rightarrow U_c$. Close enough to the isotropic and orbitally degenerate Mott transition at $U \lesssim U_c$, the correlated two-band metal can be driven effectively one band by a splitting as small as the Kondo energy scale $\Delta \propto zW$. The one-band metal, in turn, has a lower U_c , so that the resulting state is an insulator.

With this model result in hand, we move on to consider $NH_3K_3C_{60}$, where we carry out a DFT-LDA electronic structure calculation to extract an order of magnitude for the effective orthorhombic splitting parameter Δ/W , found to be of order 0.25. Despite the obvious differences between the two-band Hubbard model and the true three band system, it can reasonably be expected that the orthorhombic splitting will similarly drive the initially cubic fulleride with a small quasiparticle residue z from metal to insulator. In turn, the return to metallicity of the ammoniated orthorhombic fulleride can be rationalized in terms of the phase diagram, and leads to an interesting question regarding the effective number of bands in that metal. It is finally concluded that anisotropy is probably not an irrelevant element in promoting the Mott state in this material.

This paper is organized as follows: Sec. II introduces the model and deals with its simple limiting cases. The calculation and results within the DMFT are described in Sec. III. The t_{1u} band structure of $NH_3K_3C_{60}$ and its splitting due to anisotropy is described in Sec. IV. The discussion and conclusions are finally presented in Sec. V.

II. THE MODEL

We work with the simplest two-band Hubbard model, assuming purely diagonal hoppings between orbitals on different sites, the anisotropic symmetry lowering all embodied in a diagonal on-site splitting term. We write the Hamiltonian as:

$$H = -t \sum_{\langle i,j \rangle, \sigma} \sum_{\alpha=1,2} \left(c_{i\alpha\sigma}^\dagger c_{j\alpha\sigma} + H.c. \right) + \sum_i \sum_{\alpha=1,2} \epsilon_\alpha n_{i\alpha} + \frac{U}{2} \sum_i n_i(n_i - 1), \quad (1)$$

where $c_{i\alpha\sigma}^\dagger$ creates a spin- σ electron in orbital α at site i , $n_{i\alpha} = \sum_\sigma c_{i\alpha\sigma}^\dagger c_{i\alpha\sigma}$, $n_i = \sum_\alpha n_{i\alpha}$ is the total number of electrons at site i , and $\langle i, j \rangle$ denotes nearest-neighbor sites. The first term is a standard tight-binding first-neighbor hopping, simplified to ignore non diagonal hopping, and also merohedral disorder, both of them present in the real systems. The second term introduces the anisotropic splitting Δ as a shift of the on-site orbital energy $\epsilon_2 = -\epsilon_1 = \Delta/2$. The last term is the Hubbard on-site interaction, which we take in its simplest form, omitting for example any additional intra-site Hund's rule interaction terms. We also ignore the on-site electron-vibron couplings and the ensuing Jahn-Teller effects, even if quite important for other aspects [19,20].

In the $U = 0$ limit, the splitting $\Delta > 0$ simply operates a rigid shift of band 2 upwards with respect to band 1, promoting electron transfer from the upper to the lower band. Above a critical value $\Delta = \Delta_c$, and for a total electron filling $n < 2$, the upper band is emptied up. For example, with two symmetric bands of width W and $n = 1$ electrons per site, the upper band is emptied above $\Delta_c/W = 0.5$. At zero temperature (where we shall restrict ourselves in this paper) and zero interaction, $U = 0$, the transition between the “two-band metal” and the “one-band metal” is continuous. Because the topology of the Fermi surface changes, this transition is accompanied by a weak singularity of the total energy first described by Lifshitz [21]. When the electron-electron interaction U is turned on, one expects the emptying of the upper band to take place at smaller values of Δ_c , owing to the effective band narrowing. Perturbatively in U one can show that

$$\Delta_c(U) = \Delta_c(0) - \gamma U + O(U^2), \quad (2)$$

where the value of the coefficient $\gamma > 0$ depends on details of the bands. In addition, electron-electron interactions might modify the nature of the metal-metal transition singularity relative to the non-interacting case [22], a point which we will not further address here.

We restrict to a filling of one electron per site, $n = 1$, discarding the trivial case $n = 2$ where the large- Δ state is a band insulator, as well as noninteger n , where insulators are not possible. The $\Delta = 0$ and $\Delta \rightarrow \infty$ limits then reduce respectively to the (quarter-filled) two-band and the (half-filled) single-band Hubbard models, both possessing a metal-insulator transition as a function of U [18,23–25].

The limit of strong interaction $U \gg W$ is insulating for any value of Δ . This limit can be studied by mapping the model (1) onto a spin and orbital exchange Hamiltonian [26]

$$H_{\text{exch}} = J \sum_{\langle i,j \rangle} (\mathbf{S}_i \cdot \mathbf{S}_j + \mathbf{T}_i \cdot \mathbf{T}_j + 4 \mathbf{S}_i \cdot \mathbf{S}_j \cdot \mathbf{T}_i \cdot \mathbf{T}_j) - \Delta \sum_i T_i^z \quad (3)$$

where the pseudospin-1/2 operators $\mathbf{T}_j = 1/2 \sum_{\alpha\beta\nu} c_{j\alpha\nu}^\dagger \boldsymbol{\sigma}_{\alpha\beta} c_{j\beta\nu}$ represent the orbital degrees of freedom, and $J = 2t^2/U$. For $\Delta = 0$ this model has been studied both in one [27] and two dimensions [28], with suggestions that interesting spin-liquid physics could be realized. For our purposes, it suffices to note that the model has no ferro-orbital instability, and has therefore a finite $q = 0$ orbital susceptibility. As a consequence it takes a nonzero value of Δ to fully orbitally polarize the ground state. Due to the absence of cross-band terms in the kinetic energy, complete orbital polarization occurs at a finite $\Delta_c \propto J = 2t^2/U$. For $\Delta \geq \Delta_c$ that ground state is represented by a one band Mott insulator plus a totally empty split-off band.

III. PHASE DIAGRAM

We have now all the elements to illustrate the general layout, sketched in Fig. 1, of the zero temperature phase diagram of model (1) as a function of (U, Δ) for $n = 1$ electron per site. The metal-insulator transition for $n=1$, $d = 2$ and $\Delta = 0$, previously studied in DMFT by quantum Monte Carlo [18], was found at $U_c^{2\text{-band}} \approx 1.5 W$ at the relatively low temperature $T = W/32$. The same transition with $n = 1$ in the one-band model ($d = 1$, or $d = 2$ at $\Delta = \infty$) has been similarly calculated at $U_c^{1\text{-band}} \approx 1.3 W$ also at $T = W/32$ [23]. Finite temperature of course must affect somewhat these numerical values, but a common feature with our zero-temperature DMFT calculation described below, is that $U_c^{2\text{-band}} > U_c^{1\text{-band}}$. The AB line in Fig. 1, representing U_c as a function of Δ and separating metals from Mott insulators, indicates this trend. The DM' line separates the fully orbitally polarized Mott insulator (at the right) from the two-band insulator, roughly as $U_c \sim \Delta^{-1}$ for small Δ . Similarly, the CM line separates the fully orbitally polarized metal from the two-band metal: it starts from point C with a linear slope $-\gamma^{-1}$, according to Eq. (2). In the region of full orbital polarization the value of Δ is irrelevant, and this is the reason why the Mott transition line MB is horizontal. As Δ increases, for $U < U_c^{1\text{-band}}$ the upper-band emptying transition takes the two-band metal across the CM line over to a one-band metal, while for $U > U_c^{1\text{-band}}$ it leads across the AM line to a Mott insulating state. The AM line starts off linearly at small Δ . Basically, this occurs since in close proximity of the Mott transition the relevant energy scale, to be matched by the orbital splitting Δ , is no longer the bare bandwidth, but rather the width of the Kondo-like quasiparticle peak of the correlated metal. That in turn is of the order of zW , which is smaller than W and proportional to the quasiparticle residue z , linearly vanishing with $(U_c^{2\text{-band}} - U)$ at the Mott transition [29]. As the DMFT calculations will show, the effective emptying transition occurs when Δ increases to reach $\Delta_c(U) \propto zW \propto (U_c^{2\text{-band}} - U)$.

The purpose of the DMFT calculations is to investigate this phase diagram in greater quantitative detail, in particular in the region of intermediate $U \sim W$ and $\Delta \lesssim W$. We have implemented DMFT in the exact diagonalization flavor [24,29] for the degenerate Hubbard model restricted to paramagnetic states [30]. The results of the DMFT calculations are summarized in Fig. 2.

The values we obtain for $U_c^{1\text{-band}} \simeq 1.35 W$ and $U_c^{2\text{-band}} \simeq 1.8 W$, associated to the disappearance of the metallic state for one and two bands respectively, have been calculated with the same number of discretized bath levels per band $n_b = 4$. The associated error bar is estimated by repeating the calculation with $n_b = 5$. These values are in substantial agreement with corresponding values obtained by other methods [18,23–25]. The other points in the phase diagram are obtained by following the stability of the two-band metal for a given value of U and increasing Δ , marking the emptying transition to the one-band metal or to the insulator.

A deficiency of this DMFT calculation – which is restricted as usual to paramagnetic states only – is the absence of a two-band insulating state for $\Delta > 0$. In fact the suppression of the antiferro orbital ground state of (3) produces a fictitious infinite uniform orbital susceptibility which leads to full orbital polarization as soon as Δ is turned on [29]. Despite this limitation, the results of the present calculations are suggestive, revealing the announced sharp reduction of the metal-insulator $U_c(\Delta)$ for small but finite Δ . Indeed, our calculations give a $\Delta_c(U)$ which is roughly proportional to the quasiparticle residue $z(U)$ of the undistorted ($\Delta = 0$) correlated metal at $U < U_c^{2\text{-band}}$,

$$\frac{\Delta_c(U)}{W} \propto \beta z(U), \quad (4)$$

with a proportionality constant $\beta \simeq 0.3$. Since $z(U)$ vanishes as $U \rightarrow U_c^{2\text{-band}}$, most likely linearly in $(U_c^{2\text{-band}} - U)$ [29], even a very small Δ/W can be enough to cause a metal-insulator transition in the strongly correlated metal. For example, following the bold arrow at $U = 1.5W$ in Fig. 2, a Δ value as small as $0.08W$ is sufficient to cross the transition line from the metal to insulator.

Further illustrating that, in Fig. 3 we show the behavior of the spectral density

$$A_\alpha(\omega) = -\pi^{-1} \operatorname{Im} G_\alpha(\omega) ,$$

$G_\alpha(\omega)$ being the one-particle Green's function of band α , on both sides of the metal-insulator transition. The asymmetry of the upper-band spectral density $A_2(\omega)$ (solid lines) is very pronounced, as this band is nearly ($\Delta/W = 0.07$) or completely ($\Delta/W = 0.08$) empty. As soon as the Kondo-like peaks of the two bands differ enough in energy to induce the emptying of band 2, the lower band spectral density $A_1(\omega)$ takes the symmetric shape, characteristic of the half-filled one band Hubbard model. Here the Kondo peak disappears completely, as this value of $U > U_c^{1\text{-band}}$ puts the Hubbard model of band 1 well inside the insulating regime.

IV. ANISOTROPIC BAND SPLITTING IN ORTHORHOMBIC $\text{NH}_3\text{K}_3\text{C}_{60}$

The above model calculations show that a small splitting $\Delta \propto zW$ of the orbitally degenerate band can drive the metal-insulator transition. We now wish to explore the implications that this result – if assumed to be more general than the simple model where it was derived – can have on the metal-insulator transition which takes place between isoelectronic K_3C_{60} and $\text{NH}_3\text{K}_3\text{C}_{60}$ (the former cubic and the latter orthorhombic), and on the insulator-metal transition of $\text{NH}_3\text{K}_3\text{C}_{60}$ itself under pressure.

To obtain a quantitative estimate of the actual strength of anisotropy in the ammoniated fulleride, we carried out comparative DFT-LDA electronic structure calculations for K_3C_{60} and a simplified but meaningful model of $\text{NH}_3\text{K}_3\text{C}_{60}$ using the PWSCF package based on plane waves and ultrasoft pseudopotentials [31]. We took a lattice constant $a = 14.2 \text{ \AA}$ for fcc K_3C_{60} , and $a = 14.89 \text{ \AA}$ for $\text{NH}_3\text{K}_3\text{C}_{60}$, the latter with a centered tetragonal unit cell with $c/a = 0.91$, neglecting the exceedingly small difference between a and b . In both calculations a single- C_{60} unit cell was used, as pictured in Fig. 4. In these model structures and calculations, we ignored merohedral disorder, as well as the rich antiferro-rotational structure recently discovered in actual $\text{NH}_3\text{K}_3\text{C}_{60}$ [32].

We used 27 Ry and 160 Ry plane wave energy cut-offs for the wavefunctions and the charge density, respectively. The Fermi surface was smeared with parameter of 0.3 eV and a $2 \times 2 \times 2$ Monkhorst and Pack mesh [33]. The density of states (DOS) was calculated as a sum of Gaussians of width $\sigma = 0.03 \text{ eV}$ sampling k-space with a uniform $6 \times 6 \times 6$ mesh.

Fig. 5 shows the t_{1u} bands of $\text{NH}_3\text{K}_3\text{C}_{60}$ (a), compared to those of K_3C_{60} (c); the corresponding density of states are compared in panels (b) and (d). We find that the presence of the inserted NH_3 molecules modifies only weakly the essentially pure C_{60} t_{1u} conduction band, as expected. The difference in the two band structures are almost entirely due to the different lattice structures of the molecular centers. Small changes appear in the details of the bands throughout the Brillouin Zone, but both compounds are predicted in LDA to be three-band metals, their overall t_{1u} density of states not dissimilar in the ammonia-intercalated and pristine compound. In particular, as apparent from Fig. 5(b), the bandwidths of $\text{NH}_3\text{K}_3\text{C}_{60}$ and K_3C_{60} are

close, $W \sim 0.6$ eV. The main difference in the two band structures is a splitting of the threefold degenerate t_{1u} band of K_3C_{60} at the Γ point of $\text{NH}_3\text{K}_3\text{C}_{60}$. This splitting is precisely a measure of the strength of the non-cubic crystalline environment seen by the t_{1u} orbital on each fullerene molecule in the orthorhombic structure of $\text{NH}_3\text{K}_3\text{C}_{60}$. Its magnitude is roughly a quarter (0.2 - 0.3) of the total bandwidth; that represents the main result of the calculation. If this were an uncorrelated metal, this splitting would have no major consequences, just a change of shape of the Fermi surface. The consequences can be much more important due to strong correlations, as discussed below.

V. DISCUSSION AND CONCLUSIONS

The Γ -point t_{1u} band splitting – see Fig. 5(a) – can be taken as a crude estimate of the value of $\Delta \sim 0.15$ eV in $\text{NH}_3\text{K}_3\text{C}_{60}$, corresponding to a dimensionless ratio $\Delta/W \sim 0.25$. This value is of course too small to determine a complete emptying of one of the bare, uncorrelated bands, and indeed all three bands of $\text{NH}_3\text{K}_3\text{C}_{60}$ still cross the Fermi energy E_F . However, correlations play an important role in fullerides, where the value of U is believed to lie between 1 and 1.6 eV [34], thus substantially larger than the bandwidth W . As the non-ammoniated fullerides A_3C_{60} are still generally in the metallic and superconducting phase, it is not unreasonable to assume that their value of U/W is in all likelihood only marginally smaller than the $U_c^{3\text{-band}}$ for the Mott transition in the half-filled $d = 3$ -band cubic system. Indirect evidence that ordinary, uncorrelated electronic bands do not exist, and that the electron spectral function at E_F can more reasonably be assimilated to a narrow, dispersionless Kondo-like resonance was provided for K_3C_{60} by recent photoemission data [35].

Assuming for the $d = 3$ fullerides a behavior as a function of anisotropy similar to that of the $d = 2$ model found in Secs. II and III, we can suppose that in the appropriate (U, Δ) phase diagram (Fig. 6) the ammoniation of K_3C_{60} into orthorhombic $\text{NH}_3\text{K}_3\text{C}_{60}$ could correspond to a displacement [36] similar to that of Fig. 2. Inspection of Fig. 2 shows that, if U is close enough to U_c , even a value of Δ substantially smaller than that estimated for $\text{NH}_3\text{K}_3\text{C}_{60}$ could suffice to drive that metal insulator transition.

We should stress that this picture does not exclude a role, in the metal-insulator transition, for the accompanying ammoniation-driven expansion of the lattice. That role is experimentally proven by the pressure-driven insulator-metal transition, where $\text{NH}_3\text{K}_3\text{C}_{60}$ is transformed to a metal and a superconductor, notwithstanding the permanence of the orthorhombic structure [14]. However a new, interesting question raised in Fig. 6 is what kind of metal does one recover in $\text{NH}_3\text{K}_3\text{C}_{60}$ under pressure, whether a three-band metal like the cubic K_3C_{60} , or a new effective two-band metal. The former might in effect require a smaller deformation. It would be very interesting in this regard if the Fermi-surface topology of $\text{NH}_3\text{K}_3\text{C}_{60}$ could be studied under pressure.

Another interesting – even if maybe not practically straightforward – test of this overall picture could be obtained by applying uniaxial stress to cubic superconducting fullerides of the A_3C_{60} family. Contrary to standard tendency of hydrostatic pressure toward metallization and lower superconducting T_c , the orbital splitting associated with the appropriate uniaxial strain could drive some of these compounds perhaps first toward higher T_c , and eventually Mott insulating.

In summary, we have investigated the role of a symmetry-breaking orbital splitting on the transition to a Mott insulating state in an initially orbitally degenerate strongly correlated multi-band metal. The calculations, carried out in a highly idealized $d = 2$

model, have unveiled the Kondo quasiparticle energy scale as that which the non-cubic splitting magnitude must reach in order to induce the Mott transition even at constant bandwidth and effective Coulomb repulsion. The likely relevance of this main qualitative finding to the fullerides K_3C_{60} and $NH_3K_3C_{60}$ has been highlighted.

ACKNOWLEDGMENTS

We are indebted to O. Gunnarsson and M. Fabrizio, for useful discussions. R. Assaraf collaborated with this project in its earliest stage. This work was partly supported by the European Union, contract ERBFMRXCT970155 (TMR Fulprop), and by MIUR COFIN01, MURST COFIN99.

[1] V. Brouet, H. Alloul, F. Quere, G. Baumgartner, and L. Forro, Phys. Rev. Lett. **82**, 2131 (1999).

[2] A. P. Ramirez, Supercond. Review **1**, 1 (1994).

[3] J. H. Schön, Ch. Kloc, R. C. Haddon, and B. Batlogg, Science **288**, 656 (2000).

[4] J. H. Schön, C. Kloc, and B. Batlogg, Nature **408**, 549 (2000).

[5] M. Fabrizio and E. Tosatti, Phys. Rev. B **55**, 13465 (1997).

[6] M. Capone, M. Fabrizio, P. Giannozzi, and E. Tosatti, Phys. Rev. B **62**, 7619 (2000).

[7] P. J. Benning, F. Stepniak, and J. H. Weaver, Phys. Rev. B **48**, 9086 (1993).

[8] V. Brouet, H. Alloul, T.N. Le, S. Garaj, L. Forro, Phys. Rev. Lett. **86** 4680 (2001).

[9] M. J. Rosseinsky, D. W. Murphy, R. M. Fleming, and O. Zhou, Nature **364**, 425 (1993).

[10] T. Takenobu, T. Muro, Y. Iwasa, and T. Mitani, Phys. Rev. Lett. **85**, 381 (2000).

[11] T. T. Obu, H. Shimoda, Y. Iwasa, T. Mitani, M. Kosaka, K. U. Tanigaki, C. M. Brown, and K. Prassides, Mol. Cryst. Liq. Cryst. **340**, 599 (2000).

[12] H. Tou, N. Muroga, Y. Maniwa, H. Shimoda, Y. Iwasa, and T. Mitani, Physica B **281**, 1018 (2000).

[13] O. Zhou, T. T. M. Palstra, Y. Iwasa, R. M. Fleming, A. F. Hebard, P. E. Sulewski, D. W. Murphy, and B. R. Zegarski, Phys. Rev. B **52**, 483 (1995).

[14] S. Margadonna, K. Prassides, H. Simoda, Y. Iwasa, and M. Mézouar, Europhys. Lett. **56**, 61 (2001).

[15] O. Gunnarsson, E. Koch, and R. M. Martin, Phys. Rev. B **54**, R11026 (1996).

[16] E. Koch, O. Gunnarsson, and R. M. Martin, Phys. Rev. B **60**, 15714 (1999).

[17] The origin of the band splitting at the Γ point is twofold: (i) the hopping between neighbor fullerene balls is different for pairs of molecules separated by different distances, along different crystal directions; (ii) different orbitals in the molecular t_{1u} manifold composing the conduction band acquire a different energy according to their orientation relative to the neighboring C_{60}^{3-} , NH_3 and K^+ species, forming the orthorhombic local environment.

[18] M. J. Rozenberg, Phys. Rev. B **55**, R4855 (1997).

[19] M. Capone, M. Fabrizio, E. Tosatti, Phys. Rev. Lett. **86**, 5361 (2001).

[20] N. Manini, E. Tosatti, and A. Auerbach, Phys. Rev. B **49**, 13008 (1994).

[21] I. M. Lifshitz, Sov. Phys. JETP **11**, 1130 (1960).

[22] M. I. Katsnelson and A. V. Trefilov, Phys. Rev. B **61**, 1643 (2000).

[23] M. J. Rozenberg, G. Kotliar, and X. Y. Zhang, Phys. Rev. B **49**, 10181-10193 (1994).

[24] M. Caffarel and W. Krauth, Phys. Rev. Lett. **72**, 1545 (1994).

[25] R. Bulla, Phys. Rev. Lett. **83**, 136 (1999).

[26] D. P. Arovas and A. Auerbach Phys. Rev. B **52**, 10114-10121 (1995).

[27] B. Sutherland, Phys. Rev. B **12**, 3795 (1975).

[28] Y. Q. Li, Michael Ma, D. N. Shi, and F. C. Zhang, Phys. Rev. Lett. **81**, 3527 (1998).

- [29] A. Georges, G. Kotliar, W. Krauth, and M. J. Rozenberg, Rev. Mod. Phys. **68**, 13 (1996).
- [30] Our implementation of the DMFT follows closely that of Ref. [24]. The chemical potential is adjusted at each iteration, so that the desired number of electrons per site is obtained at convergence [37]. We find advantageous to use a logarithmic mesh for the imaginary frequencies, with a low-frequency cutoff of the order of $0.02W$, to insure convergence with the rather small number of baths per band we can include ($n_b = 4 \div 5$). Our results are in substantial accord with those of the traditional linear mesh.
- [31] The package, together with the ultrasoft pseudopotentials of C, N, H and local potential of K, can be found at the URL <http://www.pwscf.org>.
- [32] S. Margadonna, K. Prassides, H. Shimoda, T. Takenobu, Y. Iwasa, Phys. Rev. B **64** 132414 (2001).
- [33] H. J. Monkhorst and J. D. Pack, Phys. Rev. B **13**, 5188 (1974).
- [34] O. Gunnarsson, Rev. Mod. Phys. **69**, 575 (1997).
- [35] A. Goldoni, L. Sangaletti, M. Peloi, F. Parmigiani, G. Cornelli, G. Paolucci, Surf. Science **482**, 476 (2001).
- [36] Polarization screening of the on-site interaction U is different in the two compounds, with poorer screening in $\text{NH}_3\text{K}_3\text{C}_{60}$ leading to a larger effective U/W . However, a crude estimate suggests that the reduced screening of C_{60} due to the slightly larger cell volume is probably over-compensated by the extra screening due to ammonia. As a net result, we expect the effective U to be substantially the same in the two compounds, as indeed seems to be the case in different fullerenes.
- [37] T. Costi and N. Manini, in print on J. Low Temp. Phys. (March 2002) - cond-mat/0109357.

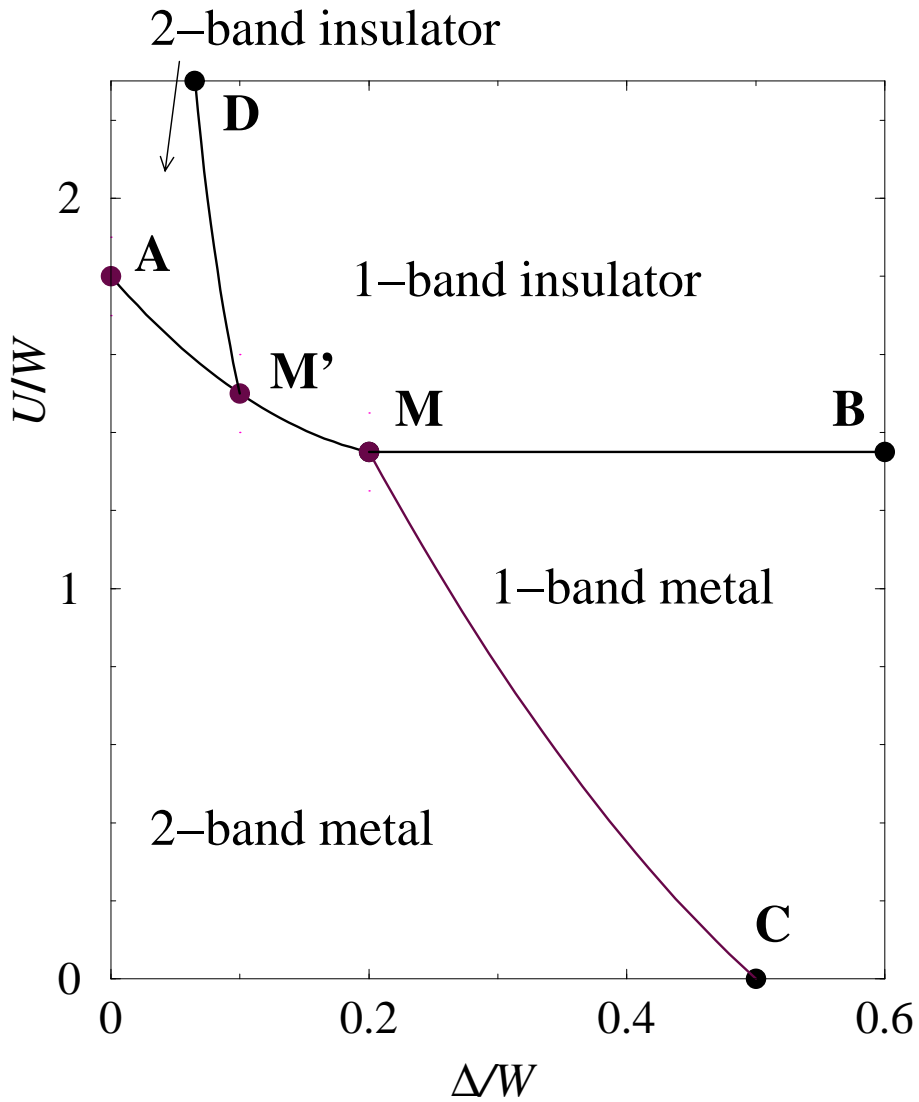


FIG. 1. Qualitative zero-temperature phase diagram for the two-band Hubbard model at quarter filling (one electron per site) in the U - Δ plane, where Δ is the anisotropy splitting of the two orbitals. The various phases and lines are described in Sect. III. The multicritical points M and M' are not necessarily distinct.

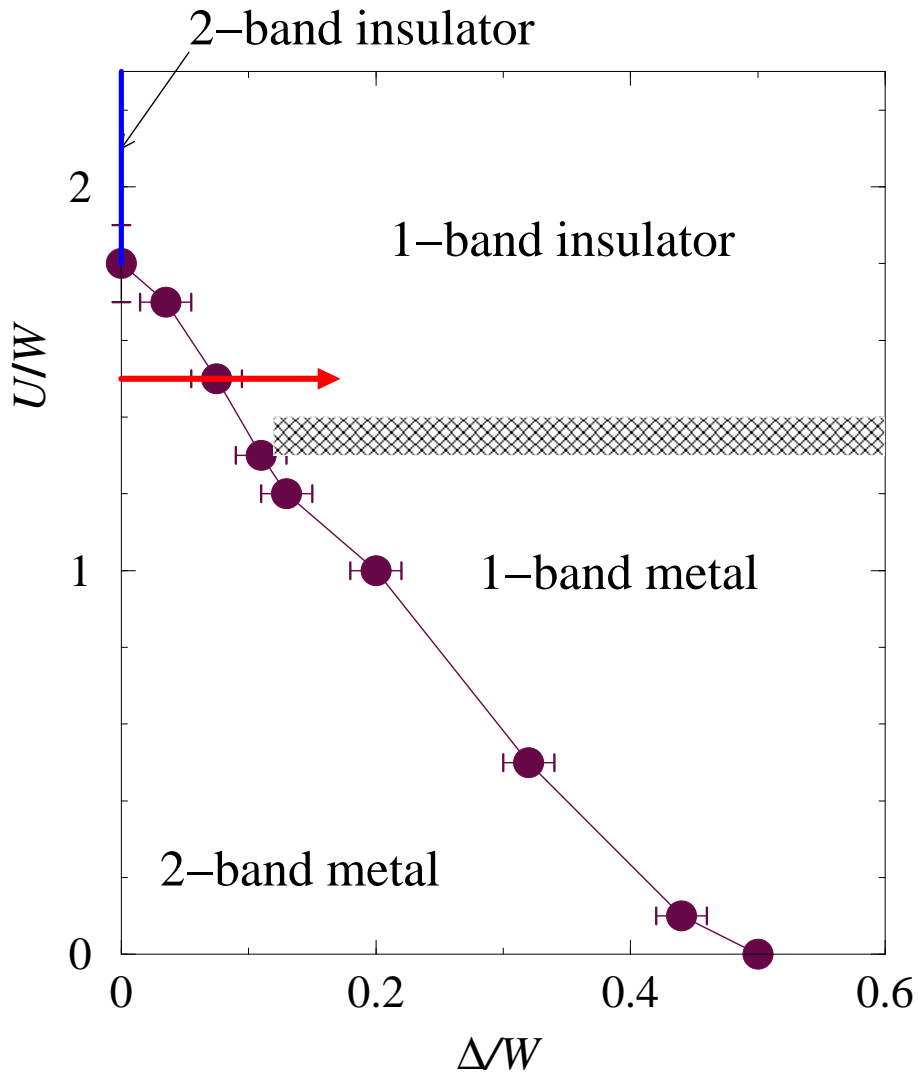


FIG. 2. DMFT zero-temperature phase diagram for the two-band Hubbard model at quarter filling (one electron per site), obtained by the exact diagonalization method in the paramagnetic sector. The discretization of the conduction band uses here $n_b = 4$ bath states per orbital degree of freedom.

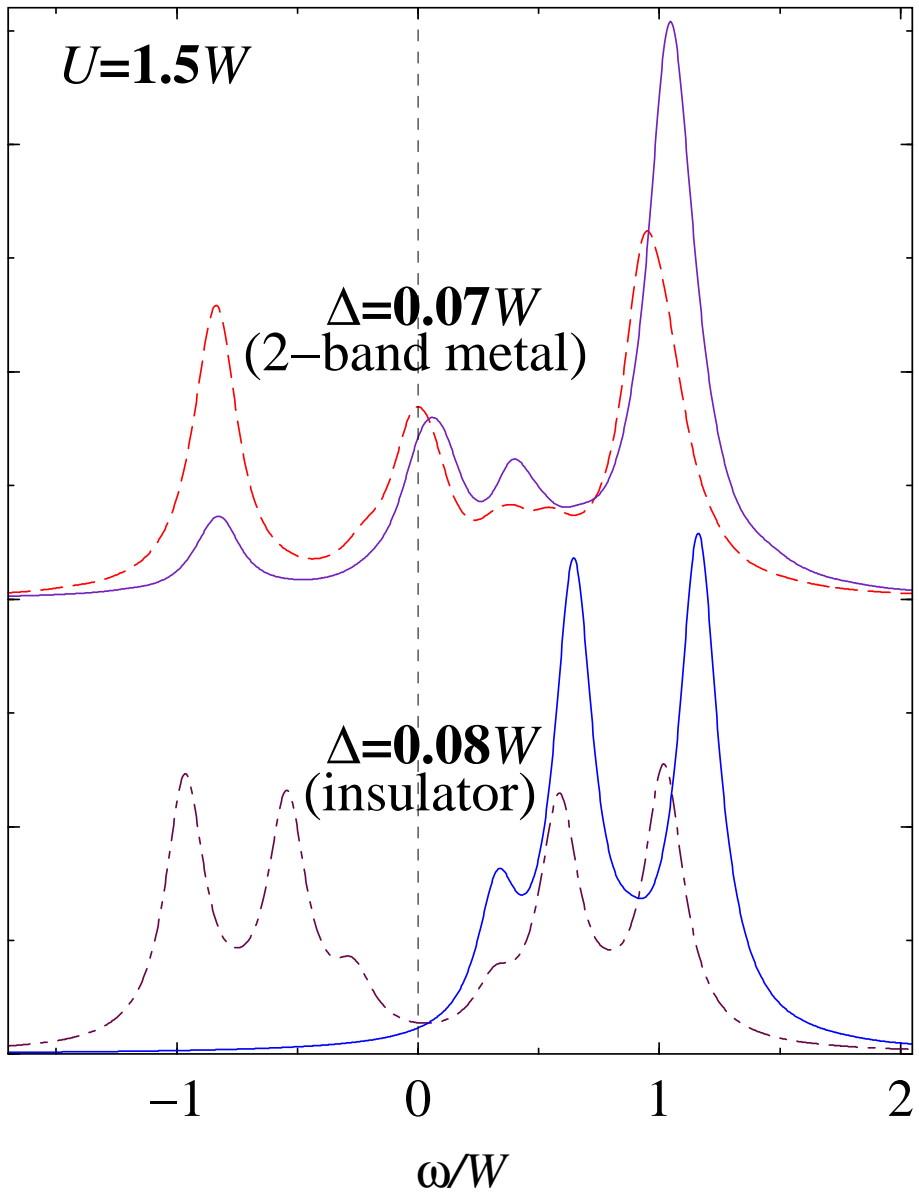


FIG. 3. Spectral density $A_2(\omega) = -\pi^{-1}\text{Im } G_2(\omega)$ at $U/W = 1.5$ across the Mott-Hubbard transition for increasing anisotropy splitting Δ . ω is referred to the Fermi energy. Solid lines refer to the minority orbital $\alpha = 2$. The multi-peak structures of the high-energy side bands are artifacts of the finite discretization of the conduction band.

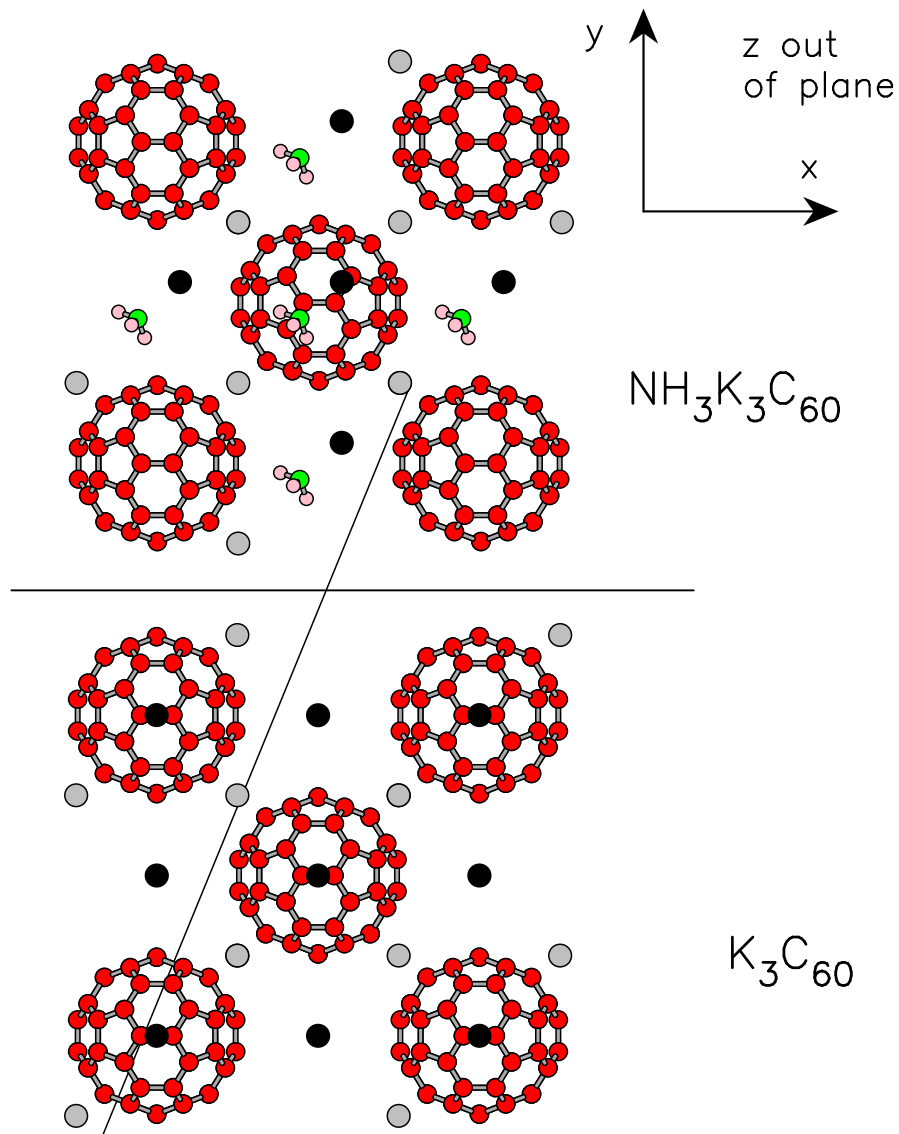


FIG. 4. Simplified geometry of $\text{NH}_3\text{K}_3\text{C}_{60}$ (top) and K_3C_{60} (bottom) used in the LDA calculation. Octahedral K atoms are indicated in black, while tetrahedral ones are in gray. All visible atoms of the central unit cell are shown together with some atoms in the neighbor unit cells. In $\text{NH}_3\text{K}_3\text{C}_{60}$ the z axis is the c -axis.

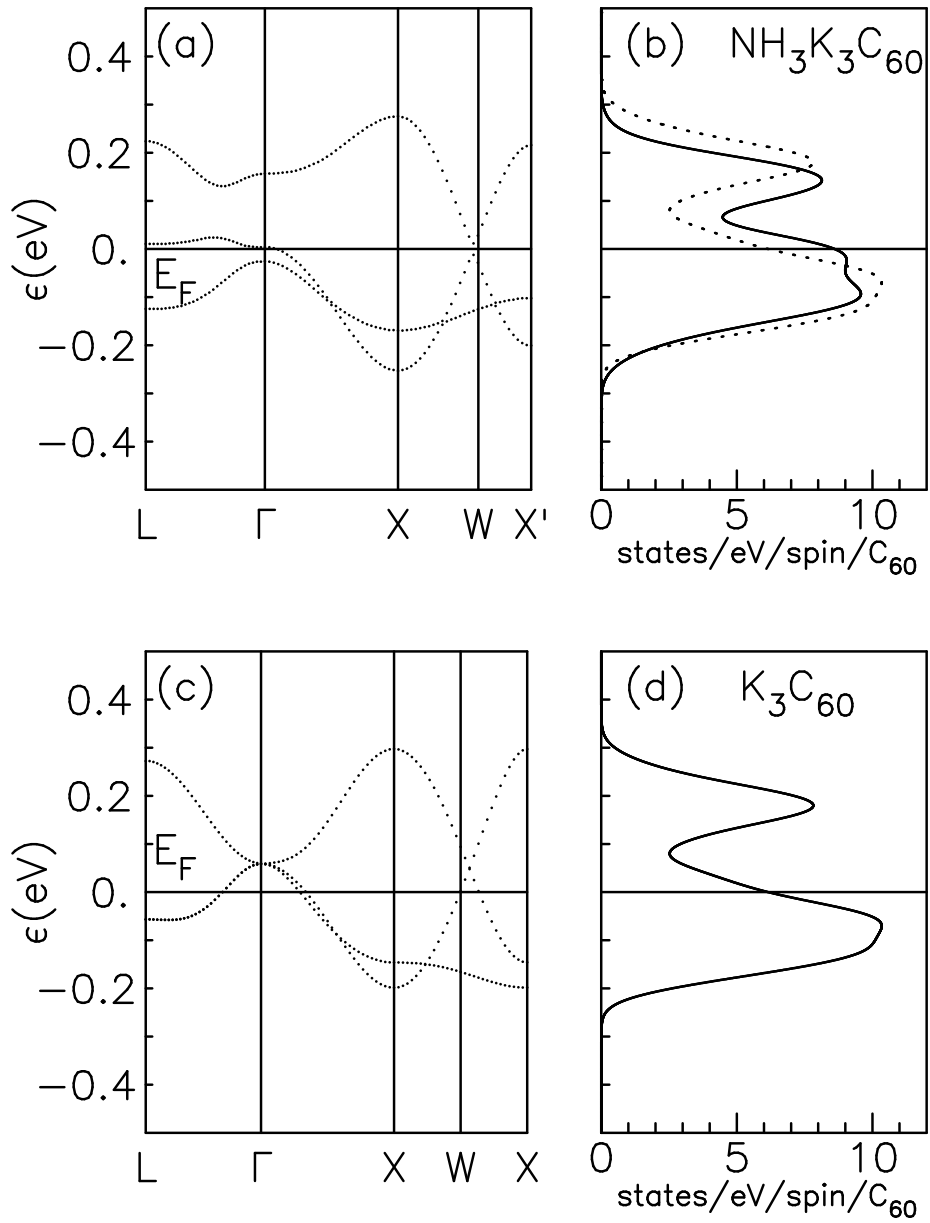


FIG. 5. Band structure of $\text{NH}_3\text{K}_3\text{C}_{60}$ (a), obtained by an LDA-DFT calculation, compared to that of K_3C_{60} (c). The corresponding densities of states are given in panels (b) and (d). In panel (b) the density of states of K_3C_{60} (dashed line) is re-drawn for direct comparison with that of $\text{NH}_3\text{K}_3\text{C}_{60}$ (solid line).

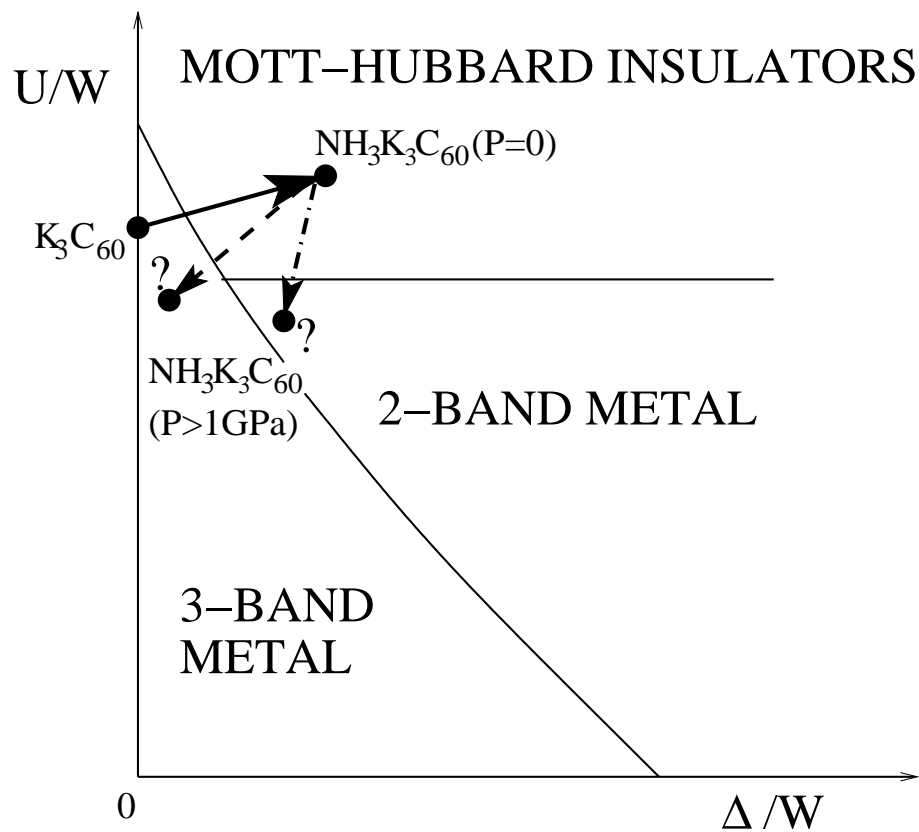


FIG. 6. A schematic (U, Δ) phase diagram for the $d = 3$ -bands family of compounds K_3C_{60} and $NH_3K_3C_{60}$. The dashed and dot-dashed arrows indicate two plausible paths of pressure-induced metallization of $NH_3K_3C_{60}$.